$(CN)_2]Br$ (T_c = 11.6 K) and κ-$(ET)_2Cu[N(CN)_2]Cl$ (T_c = 12.5 K, 0.3 kbar), respectively. As in the case of κ-$(ET)_2Cu[N(CN)_2]Br$, our band electronic structure calculations[6] show κ-$(ET)_2Cu[N(CN)_2]Cl$ to be a two-dimensional metal. Structure-properties correlations for κ-phase superconductors are now within reach and await the discovery of another isostructural superconducting salt. Extrapolation of T_c to ambient pressures for κ-$(ET)_2Cu[N(CN)_2]Cl$ indicates a T_c of ~13.2 K, and efforts are underway to stabilize this material in the superconducting ground state at ambient pressure.

Note Added in Proof. Four-probe resistance measurements with a Nb reference thermometer in series with the sample give T_c = 12.8 K at 0.3 kbar. We define T_c as the midpoint of the transition. The total transition width is less than 0.2 K at this pressure.

Acknowledgment. Work at Argonne National Laboratory, Sandia National Laboratories, and North Carolina State University is supported by the Office of Basic Energy Sciences, Division of Materials Sciences, U.S. Department of Energy, under Contracts W-31-109-ENG-38 and DE04-76DP00789 and Grant DE-FG05-86ER45259, respectively. L.K.M. and G.J.P. are Faculty Research Participants, sponsored by the Argonne Division of Educational Programs, from the Departments of Chemistry, Indiana University, Bloomington, IN, and Kent State University, Kent, OH. D.M.W., J.M.K., S.J.B., and A.V.S.C. are undergraduate student research participants also sponsored by the Argonne Division of Educational Programs from Florida Institute of Technology, Melbourne, FL; Montana State University, Bozeman, MT; Eastern Nazarene College, Wollaston, MA; and Aurora University, Aurora, IL, respectively.

Chemistry and Materials Science Divisions
Argonne National Laboratory
Argonne, Illinois 60439

Jack M. Williams*
Aravinda M. Kini*
Hau H. Wang*
K. Douglas Carlson*
Urs Geiser*
Lawrence K. Montgomery
Gloria J. Pyrka
Diana M. Watkins
Jefferson M. Kommers
Scott J. Boryschuk
Anneliese V. Strieby Crouch
W. K. Kwok*

Sandia National Laboratories
Albuquerque, New Mexico 87185

J. E. Schirber*
D. L. Overmyer

Department of Chemistry
North Carolina State University
Raleigh, North Carolina 27695-8204

D. Jung
Myung-Hwan Whangbo*

Received July 11, 1990

Articles

Contribution from Ames Laboratory—DOE[1] and the Department of Chemistry, Iowa State University, Ames, Iowa 50011

Chemistry in the Polar Intermetallic Host Zr_5Sb_3. Fifteen Interstitial Compounds

Eduardo Garcia and John D. Corbett*

Received November 23, 1989

Reactive (powder) sintering, arc-melting, vapor-phase-transport, and metal-flux methods have been explored for the synthesis of single-phase samples of compounds Zr_5Sb_3Z, in which an interstitial atom Z is bound in the centers of all zirconium trigonal-antiprismatic sites in the Zr_5Sb_3 host (Mn_5Si_3 type). Products of arc-melting are generally the least satisfactory as they are often substitutionally disordered or inhomogeneous and exhibit distinctly smaller lattice constants. Other procedures are described for the preparation of usually single-phase samples with Z = C, O, Al, Si, P, S, Co, Ni, Cu, Zn, Ge, As, Se, Ru, and Ag. The structures of two metal-flux products have been determined by single-crystal X-ray means ($P6_3/mcm$, Z = 2): Zr_5Sb_3Si, a = 8.5409 (5) Å, c = 5.8248 (7) Å, R/R_w = 2.1/3.0%; Zr_5Sb_3Zn, a = 8.6074 (7) Å, c = 5.8362 Å, R/R_w = 1.3/1.3%. The bonding of Z results primarily in small to moderate expansions of the relatively large zirconium cavity. The results of extended Hückel band calculations for Zr_5Sb_3 and Zr_5Sb_3S show how zirconium states and electrons are diverted from the broad conduction band to form strong Zr-Z bonds while the robust Zr-Sb and Zr-Zr bonding elsewhere in the structure is virtually unaffected.

Introduction

Cluster phases constructed from the early transition metals (T) exhibit some unusual and distinctive solid-state chemistries. The simplest to understand, and the most polar, are the many discrete cluster halides (X) formed from T_6X_{12} units. Metal-rich binary compounds formed between the same metals and the earlier chalcogens, pnictogens, and other main-group elements (M) still involve components with quite different valence-state energies, and the assignment of valence electrons to valence and conduction (or cluster) bands is usually quite straightforward.[2] However, the smaller fraction of M atoms means that even the binary compounds frequently occur in structures that are so condensed and complex that it is difficult to understand and discuss their structures, bonding, and chemistry directly without a theoretical band elaboration of each phase. Further reactions of most of these to form related ternary phases, interstitial or not, have not been systematically investigated beyond a few carbides, hydrides, etc.

Cluster halides constructed from group 3 or 4 metals have recently been found to exhibit a surprising property: all evidently require an interstitial element centered within each metal octahedron for thermodynamic stability.[3-5] Paralleling this, some metallic chalcogenide, pnictide, etc. phases with relatively simple cluster-based structures have been found to exhibit evidently analogous reactions. In these cases, a variety of third elements are taken up interstitially and without large structural changes so that electronic changes accompanying the reactions are easier to understand. The term "Nowotny phase" has been applied to some of these.[6]

One particular family, T_5M_3 phases with the Mn_5Si_3-type structure, have a longstanding reputation for their ability to bond a third interstitial element (Z) within T_6 octahedral cavities therein, or even to require the same for stability.[7-11] In fact, some

(1) Ames Laboratory—DOE is operated for the U.S. Department of Energy by Iowa State University under Contract No. W-7405-Eng-82. This research was supported by the Office of Basic Energy Sciences, Materials Sciences Division.
(2) Garcia, E.; Corbett, J. D. *Inorg. Chem.* **1988**, *27*, 2353.
(3) Ziebarth, R. P.; Corbett, J. D. *Acc. Chem. Res.* **1989**, *22*, 256.
(4) Rogel, F.; Zhang, J.; Payne, M. W.; Corbett, J. D. *Adv. Chem. Ser.* **1990**, *226*, 369.
(5) Payne, M. W.; Corbett, J. D. *Inorg. Chem.* **1990**, *29*, 2246; see also references therein.
(6) Kieffer, R.; Benesovsky, F.; Lux, B. *Planseeber.* **1956**, *4*, 30.

0020-1669/90/1329-3274$02.50/0

binary phases reported with this structure were probably ternary compounds stabilized by common impurities, especially C, N, or O. However, much of the past work has only been qualitative. Synthetic routes to single-phase examples of the ternary compounds as well as their stoichiometries and structures have been quantified in only a very few cases, and none systematically insofar as the range of Z possible.

The present study deals with Zr_5Sb_3, a long-known[12] example of this structure and reactivity. One early investigation concluded that this compound was actually Zr_5Sb_3O with oxygen as a necessary third component, the evidence for this being mainly that the volume per atom at this composition was 4.5% greater than that in other Zr–Sb binary phases then known.[13] Other ternary Zr_5Sb_3Z compounds were later reported to be formed in powder sintering reactions at 800 °C, namely for Z = Ni, Cu, and Zn, while B, C, Mn, Fe, Co, Ru, Ir, and Pt were stated not to form such phases.[14] The contrast between the oxygen and Ni–Zn examples seemed especially remarkable to us. We first investigated the binary system in the neighborhood of Zr_5Sb_3 to establish that this simple compound does exist. In addition, a nonstoichiometry region involving the self-interstitial antimony and with characteristic changes in lattice dimensions was found to extend up to about $Zr_5Sb_{3.4}$ in the neighborhood of 1100 °C.[2] Interestingly, the lattice constants we determined for the approximate compositions $Zr_5Sb_{3.12}$ and $ZrSb_{3.3}$ correspond well to those reported previously for Zr_5Sb_3[12] and Zr_5Sb_3O.[13] Similar cell volumes, although somewhat different c/a ratios, were cited for the above Ni, Cu, and Zn examples.

Our investigations of Zr_5Sb_3Z systems set out to establish reliable methods for the synthesis of ordered, single-phase samples of such compounds as well as to explore the breadth of the interstitial chemistry. This led to broad explorations of powder-sintering, arc-melting, vapor-phase-transport, and metal-flux methods for synthesis and to the identification of at least 15 examples of compound formation with heteroatomic Z. The value of single-crystal studies in establishing compositions as well as dimensions has led to investigations of several examples from both arc-melted and fluxed reactions. These and the synthetic results have brought us to the general conclusion that arc-melting is deficient in several respects in providing well-defined, equilibrium samples. A few extended Hückel band calculations have also been carried out in order to examine both the bonding in the ternary phases and the unprecedented versatility of these systems insofar as the wide variety of interstitials that can be encapsulated.

Experimental Section

Materials. The reactor grade zirconium and reagent grade antimony utilized, the preparation of powdered samples of each, and the arc-melting procedures have been described previously.[2,15] Powdered Zr_5Sb_3 was prepared by grinding an arc-melted sample of that composition. Sources of the other reactants: C, Union Carbide, spectroscopic grade; Al, United Mineral and Chemical, high purity; Si and Ge, Johnson-Mathey, zone-refined; P (red), J. T. Baker; S, Alfa Products, 99.999%; Cr and Mn, A. D. MacKay, 99.9%; Fe, Plastic Metals, 99.9%; Co, Alfa Products, 99.5%; Ni and Cu, J. T. Baker, 99.9 and 99.99%, respectively; Zn, Fisher Scientific (filtered through a frit); As, Alfa Products, 99.9999%; Se, American Smelting and Refining, 99.999%; Ag, G. F. Smith Chemical Co., reagent; Ru, Engelhard Industries, 99.5%.

Syntheses. All powdered or ground reagents were handled only in a glovebox. Mixtures for reactive (powder) sintering were pressed into pellets (typically 13 mm in diameter, 1–2 mm thick) at 8 kbar. Generally, the pellets were sealed within heliarc-welded Ta tubing under inert conditions if the sintering temperature was to be above 1100 °C; otherwise, the pellets were wrapped in Ta foil and sealed in fused-silica containers under ~100 Torr of argon. The reactants $CoSb_3$ and $CuSb_3$ (=Sb + Cu_2Sb) were prepared by heating the appropriate mixture of the elements in an alumina crucible at 1000 or 750 °C, respectively. Each produced a brittle material that could be easily ground prior to reaction with zirconium. Sintering reactions of pressed pellets made with elemental P, As, S, or Se are not practical because of their volatility. Instead, a finely powdered Zr_5Sb_3 was allowed to react with the gaseous pnictogen or chalcogen by slowly heating these in a sealed Ta tube from room temperature to 1300 °C in 18 h. The reaction container remained ductile, indicating that the non-metal had reacted with the Zr_5Sb_3 and not the tantalum. In the case of phosphorus, the Zr_5Sb_3 was allowed to react with the phosphorus at 650 °C in a sealed SiO_2 container without any attack of the container. This material was then ground, pelletized, and sintered at 1300 °C with satisfactory results.

Powder sintering or other formation reactions were usually completed in Ta containers at 1300 or 1350 °C in ~3 days in an evacuated tube furnace. Early work utilized a mullite tube furnace in which a vacuum of 10^{-5} atm could be attained, but this usually resulted in appreciable amounts of ZrO_2 (and therefore excess Sb) in the products. A recrystallized alumina tube was later employed in a graphite-heated furnace that allowed evacuation to 10^{-6} atm and resulted in, at most, traces of ZrO_2.

Quantitative syntheses of Zr_5Sb_3Si and Zr_5Sb_3Zn were achieved in Zn-fluxed reactions of the powdered elements at 900 and 1000 °C, respectively. A 20-fold excess of zinc was employed in an Al_2O_3 crucible sealed under Ar within a fused silica jacket. After 6–7 days, all of the excess zinc had evaporated from the crucible into the cooler portions of the jacket.

In general, Zr_5Sb_3Z compounds are not sensitive toward moisture, and in fact most are not appreciably attacked by dilute solutions of mineral acids. On the other hand, they are air-sensitive, presumably because of reaction with atmospheric oxygen, with transition-metal interstitial compounds being the most reactive. The rate of decomposition in air is, of course, dependent on surface area; an arc-melted button will begin to tarnish within 1 day and will turn to an amorphous black powder on a time scale of weeks.

X-ray Studies. Customary procedures for Guinier powder diffraction and the refinement of lattice constants relative to silicon as an internal standard were employed.[2] Single-crystal rods of Zr_5Sb_3Si and Zr_5Sb_3Zn about 0.1 × 0.1 × 0.3 mm in dimensions were recovered from zinc-fluxed reactions and sealed within thin-walled capillaries in a glovebox designed for that purpose. Diffraction data for each were collected on a four-circle diffractometer at room temperature for the space group $P6_3/mcm$ (Mn_5Si_3 type) that was indicated by Guinier powder photographs. Data reduction, absorption correction, and structure refinements were routine; some summary data are given in Table I. Programs and sources of data have been referenced previously.[16]

PES. Photoelectron spectroscopic data were secured with the aid of an AEI-200B spectrometer and He I or Al Kα radiation, as described earlier.[17] Samples were mounted on an indium substrate. The binding energies of the core levels were referenced to adventitious carbon at 285.0 eV.

Extended Hückel Band Calculations. Three-dimensional calculations were carried out at 24K points as before[18] utilizing published methods

Table I. Selected Data Collection and Refinement Data for Zr_5Sb_3Z Single-Crystal Studies

	Z	
	Si	Zn
space group, Z	$P6_3/mcm$, 2	$P6_3/mcm$, 2
a, Å	8.5686 (7)	8.6074 (7) [a]
c, Å	5.7934 (8)	5.8362 (8)
2θ(max), deg	55	55
abs coeff μ, cm^{-1} (Mo Kα)	177	204
R, R_w [b]	0.021, 0.030	0.013, 0.013

[a] From refined Guinier powder data. [b] 177 and 172 independent reflections, respectively, and 17 variables; $R = \sum||F_o| - |F_c||/\sum|F_o|$. $R_w = [\sum w(|F_o| - |F_c|)^2/\sum w(F_o)^2]^{1/2}$; $w = 1/\sigma(F_o)^2$.

(7) Parthé, E.; Norton, J. T. *Acta Crystallogr.* **1958**, *11*, 14.
(8) Nowotny, H. In *Electronic Structure and Alloy Chemistry of the Transition Metals*; Beck, P. A., Ed.; Interscience Publishers: New York, 1963; p 179.
(9) Jeitschko, W.; Nowotny, H.; Benesovsky, F. *Monatsh.* **1963**, *94*, 844; **1964**, *95*, 1242.
(10) Rieger, W.; Nowotny, H.; Benesovsky, F. *Monatsh.* **1964**, *95*, 1417; **1965**, *96*, 98, 232.
(11) Pearson, W. B. *The Crystal Chemistry and Physics of Metals and Alloys*; Wiley-Interscience: New York, 1972; pp 718, 720.
(12) Boller, H.; Parthé, E. *Monatsh.* **1963**, *94*, 225.
(13) Rossteutscher, W.; Schubert, K. *Z. Metallkd.* **1965**, *56*, 813.
(14) Rieger, W.; Parthé, E. *Acta Crystallogr.* **1968**, *B24*, 456.
(15) Garcia, E.; Corbett, J. D. *J. Solid State Chem.* **1988**, *74*, 440.
(16) Hwu, S.-J.; Corbett, J. D.; Poeppelmeier, K. R. *J. Solid State Chem.* **1985**, *57*, 43.
(17) Corbett, J. D.; Meyer, G.; Anderegg, J. W. *Inorg. Chem.* **1984**, *23*, 2625
(18) Garcia, E.; Corbett, J. D. *J. Solid State Chem.* **1988**, *74*, 452.

Table II. Reactions To Produce Zr_5Sb_3Z[a]

Z	powdered reactants	method[b] (container)	T, °C	days	other products[c]
C	Zr, Sb, C	S (Ta)	1300	3	none
O	ZrO_2, Zr, Sb	S (Ta)	1300	3	ZrO_2, $Zr_5Sb_{3.4}$, $ZrSb_{1-x}$[d]
Al[d]	Zr_5Sb_3,3Li	R (Ta)	~750	10.5	
	"$Zr_5Sb_3Li_3$", AlI_3	R (Ta)	≤1100	6	none
Si	Zr_5Sb_3 + Si	S (Ta)	1300	3	none
	Zr, Sb, Si (excess Zn)	Zn flux (Al_2O_3)	900	7	none
P	Zr_5Sb_3 + P	R (SiO_2)	650	1	
		S (Ta)	1300	3	tr ZrO_2[e]
S	Zr_5Sb_3 + S	R (Ta)	25–1300	0.75	
			1300	3	none
Ge	Zr_5Sb_3 + Ge	S (Ta)	1300	3	tr ZrO_2
As	Zr_5Sb_3 + As	R (Ta)	25–1300	0.75	
			1300	3	tr ZrO_2
Se	Zr_5Sb_3 + Se	R (Ta)	25–1300	0.75	
			1300	3	none
Co	Zr, $CoSb_3$	S (Ta)	1300	3	tr ZrO_2
Ni	Zr, Sb, Ni (tr SbI_3)	T (Ta)	1150	18	none
Cu	Zr, Sb, Cu_2Sb	S (Ta)	25–1350	0.5	
			1350	3	tr ZrO_2
Zn	Zr, Sb, Zn (excess)	Zn flux (Al_2O_3)	1000	6	none
Ag	Zr, Sb, Ag (tr SbI_3)	T (Ta)	1150	19	none
	Zr, Sb, Ag	S (Ta)	1350	3	none
Ru	Zr, Sb, Ru	S (Ta/SiO_2)	1350	2	none

[a] All reactions were loaded with the stoichiometry for Zr_5Sb_3Z. [b] R = reaction of volatile component with powdered reagent; S = sintering of pressed pellet; T = transport reaction. [c] Besides Zr_5Sb_3Z. All target phase patterns were sharp; tr = trace. [d] See text. [e] One faint line from ZrO_2.

and programs.[19] Energy and orbital parameters employed for Zr and Sb were cited earlier[18] while those used for S were as follows: 3s, −20.00 eV; 3p, −13.30 eV; ξ_1 = 1.82. The iron calculation was carried to charge self-consistency, giving the following parameters: 3d, −8.73 eV; 4s, −7.40 eV.

Results and Discussion

Syntheses. Understanding the synthetic results as well as the outcome of the subsequent structural and bonding investigations requires a prior knowledge of the Zr_5Sb_3 (Mn_5Si_3-type) structure. Figure 1 shows two views of this.[2] At the top is a schematic [001] projection with the atoms shaded according to their heights in *z*. Chains of confacial Zr(2) trigonal antiprisms (smaller shaded circles) lie along 0, 0, *z*, the shared edges of these being bridged by antimony atoms that are also bonded exo to Zr(2) vertices in adjoining chains. The interstitial sites of interest are centered within the trigonal antiprisms and lie at $z = 0, {}^1/_2$. Strings of Zr(1) atoms lie along ${}^1/_3, {}^2/_3, z$, and each metal is surrounded by a distorted confacial antiprism of the above antimony atoms. The bottom part of Figure 1 shows side views of the two chains; note that the same antimony atoms are members of both chains so that the bonding is not as anisotropic as implied by this depiction.

Conditions for the successful syntheses of 15 new ternary Zr_5Sb_3Z phases, usually via powder sintering, are listed in Table II, and the lattice constants and cell volumes for these new products together with reference values for Zr_5Sb_3 and $Zr_5Sb_{3.4}$ are given in Table III. The most important criterion for success in most of these reactions is the production of a sample that has the known structure and is single phase according to its Guinier powder pattern. Although changes in powder pattern intensities should, in principle, also aid in product identification, many of these changes can be mimicked by antimony self-interstitials[2] or substitution products, and we have concluded that the lattice dimensions are more characteristic and useful. Other particulars associated with obtaining a good sample of each Zr_5Sb_3Z phase together with comparisons with a few literature citations follow. Structural results for Zr_5Sb_3Si and Zr_5Sb_3Zn and general observations regarding the inadequacy of the arc-melting synthesis of most of these ternary phases are considered thereafter.

Carbon. Sintering a pressed pellet of the elements in stoichiometric proportions produced a single phase with the Zr_5Sb_3 (Mn_5Si_3-type) structure that had distinctly smaller lattice constants and volume, strong support for the production of the ternary phase. It has been reported that this phase could not be prepared via sintering for up to 8 weeks at (only) 800 °C.[14] We found that arc-melting reactions starting with Zr, ZrC, and Sb always left substantial amounts of unconsumed ZrC and gave products with lattice constants nearly as large as for Zr_5Sb_3 (8.3828 (8), 5.7616 (9) Å). There may still be a low concentration of interstitial carbon in these materials.

Table III. Lattice Parameters (Å) and Volumes (Å^3) for Zr_5Sb_3Z Phases[a]

Z	*a*	*c*	*c*/*a*	*V*
C	8.3017 (6)	5.7126 (7)	0.688	340.95 (7)
O	8.3146 (6)	5.6954 (4)	0.685	340.99 (6)
Al	8.5802 (6)	5.8465 (8)	0.681	372.76 (8)
Si	8.5409 (5)	5.8248 (7)	0.682	367.97 (6)
P	8.462 (1)	5.813 (1)	0.687	360.4 (1)
S	8.4265 (4)	5.8999 (6)	0.700	362.80 (5)
Ge	8.5593 (5)	5.8286 (6)	0.681	369.80 (6)
As	8.5007 (5)	5.8490 (7)	0.688	366.03 (6)
Se	8.4824 (4)	5.9046 (6)	0.696	368.08 (5)
Co	8.6138 (8)	5.852 (1)	0.679	376.0 (1)
Ni	8.6004 (6)	5.8281 (7)	0.678	373.33 (7)
Cu	8.5999 (4)	5.8293 (5)	0.678	373.36 (5)
Zn	8.6074 (7)	5.8362 (8)	0.678	374.46 (8)
Ru	8.634 (1)	5.855 (2)	0.678	378.0 (2)
Ag	8.6235 (3)	5.8808 (5)	0.682	378.74 (4)
$Zr_5Sb_{3.0}$[b]	8.4177 (7)	5.766 (1)	0.685	353.81 (9)
$Zr_5Sb_{3.4}$[b]	8.5694 (6)	5.8727 (7)	0.685	373.48 (7)

[a] Least-squares fit to sharp lines in Guinier powder diffraction data with Si as internal standard; space group $P6_3/mcm$, λ = 1.540 56 Å. See Table II for reaction conditions. [b] Data from ref 2.

Oxygen. A quantitative synthesis of $Zr_5Sb_3O_x$ has not yet been successful. Sintering a pressed pellet of Zr, Sb, and ZrO_2 under the conditions listed left unreacted ZrO_2 as well as $ZrSb_{1-x}$[15] and $Zr_5Sb_{3.4}$, indicating some loss of zirconium as the oxide and, possibly, via reaction with the tantalum container. Nonetheless, the system also contained a significant amount (~50%) of a Mn_5Si_3-type phase with markedly smaller lattice constants, similar to but distinctly different from those for the carbide. We concluded that the oxide derivative had been formed. Additional grinding and reaction would doubtlessly improve the yield. Although the composition was uncertain, confirmed nonstoichiometry in Zr_5M_3Z phases with heteroatom interstitials appears to be rare at these temperatures (below). Arc-melting of the sintered product gave a 3% weight loss, and a pattern with unidentified lines as

(19) Hoffmann, R. *J. Chem. Phys.* **1963**, *39*, 1397.

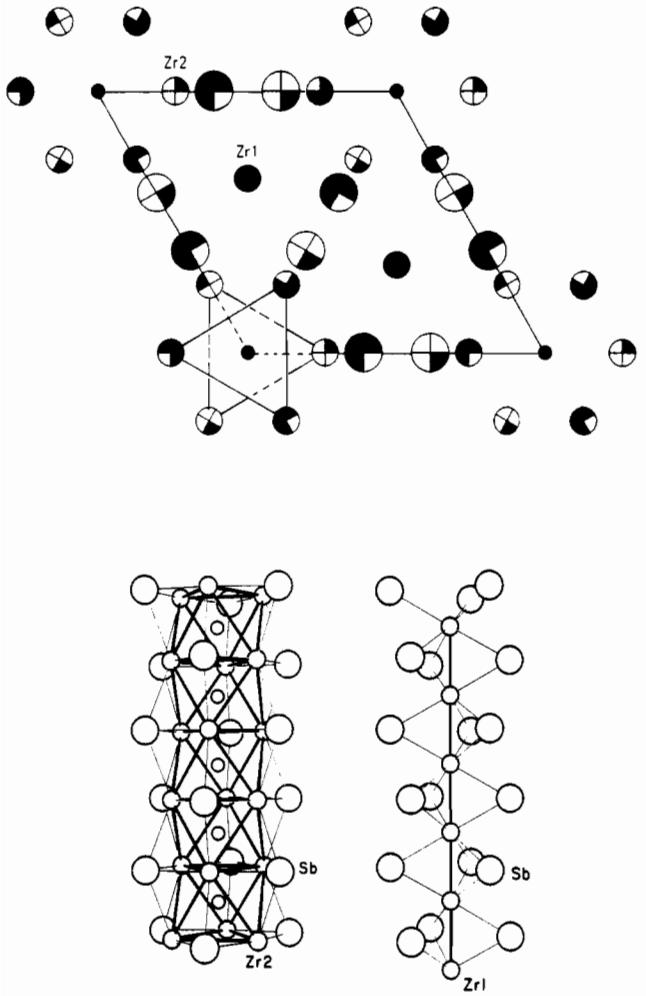

Figure 1. Top: [001] projection of the structure of Zr_5Sb_3 (Mn_5Si_3 type) with the atoms shaded according to their z coordinates: large circles, Sb; medium circles, Zr; small circle, interstitial site. Solid circles lie at z = 0 and $^1/_2$. Bottom: Side view of the confacial $[(Zr(2))_{6/2}Sb_{6/2}]$ chain (left) and the $[Zr(1)Sb_{6/2}]$ strings (right). The small open circles mark the interstitial sites in the former. Note that the same antimony atoms are members of both chains.

well as the broad lines of the hexagonal phase in the size range appropriate to Zr_5Sb_{3+x}. Cell constants of comparable magnitude (a = 8.53, c = 5.85 Å) that were reported earlier[13] for an assumed arc-melting synthesis of Zr_5Sb_3O from impurities in the reagents indicate the oxygen assignment was in error.

Aluminum. Arc-melting attempts and a single-crystal study on that product indicated the common problems of inhomogeneity, exchange, and mixed interstitials were present (below). Some of these difficulties are not surprising since extensive solid solutions between Zr_5Al_3 and Zr_5Sb_3 are known.[20] In order to avoid these, a lower temperature route involving finely divided aluminum was devised. Powdered Zr_5Sb_3 was reacted with 3 equiv of lithium, and the (presumably mixed phase) product was reground and reacted with 1 equiv of sublimed AlI_3 at slowly increasing temperatures. The LiI produced was then vacuum-sublimed from the product. The sharp pattern of the single-phase, Mn_5Si_3-type result yielded lattice constants that were larger than those from the previous arc-melting attempt, and these were concluded to be those of Zr_5Sb_3Al.

Silicon. The powder pattern of the arc-melted product contained only broad lines. Sintering of a 1:1 pelleted mixture of Zr_5Sb_3 and Si as tabulated worked well and gave single-phase Zr_5Sb_3Si with a cell somewhat smaller than that for aluminum. In order to investigate the compound more thoroughly, a quantitative yield of single crystals of the compound was also obtained with the aid of a zinc flux. One of these was characterized by X-ray diffraction means (below).

Phosphorus. In order to avoid problems associated with the vapor pressure of the element, a mixture of powdered Zr_5Sb_3 and P was first reacted in a sealed silica container, the mixed-phase product ground and pressed into a pellet, and this heated in a sealed Ta jacket at 1300 °C (1000 °C proved to be inadequate). The product showed the appropriate sharp pattern plus a trace of ZrO_2 (one weak line); the oxygen source was the furnace atmosphere—see the Experimental Section.

Sulfur. The procedure for the preparation of Zr_5Sb_3S was similar to that just given except that slow heating of a Zr_5Sb_3–S mixture to 1300 °C served to incorporate the sulfur without noticeable interference from the Ta container. The single-phase product is notable for its large c lattice constant (Table III), but the selenide behaves analogously (below). Arc-melting a mixture of a prereacted Zr_5S composition with Sb gave a product with broad lines in its pattern and distinctly smaller lattice constants. A zinc-fluxed route was not satisfactory, giving ZrS instead.

Germanium. Powder sintering of pelleted Zr_5Sb_3 and Ge gave a substantially single-phase product. Arc-melting was not tried since the existence of Zr_5Ge_3[7] suggested that some disorder between germanium and antimony sites would occur. A transport reaction was also tried, reacting ground Zr, $ZrSb_2$, and Ge in a Ta tube in the presence of ~5 mg of ZrI_4. This was heated for 1 week at 1300 °C in a tube furnace with a vacuum of marginal quality (~10^{-5} atm). The result was a microcrystalline Mn_5Si_3-type product with nicely reflective faces mixed with about 10% ZrO_2. The sharp powder pattern yielded lattice constants (8.5284 (6), 5.8186 (7) Å) that were distinctly smaller than for the sintered result. This and loss of zirconium to ZrO_2 suggest the product contained mixed Sb–Ge interstitials. The method may still be suitable under better vacuum conditions.

Arsenic. The successful synthesis paralleled that for sulfur already described.

Selenium. The successful synthesis followed that for the sulfur analogue, and a comparably large c dimension was also found. Equilibrium was not achieved in a similar reaction carried out in an alumina crucible within a fused silica jacket under 250 Torr of Ar, first at 400 °C and then at 1050 °C for 5 days.

Cobalt. The preparation of this ternary phase took into account some of the problems encountered with the ternary iron system.[21,22] The product of arc-melting this composition gave one extra line and lattice constants that were each 0.05 Å smaller, again suggesting some disorder. The formation of this compound has been reported[14] to be impossible with sintering conditions that were, with hindsight, not very satisfactory for the production of the following three compounds either.

Nickel. Since single crystals were desired, a mixture of the elements were sealed in Ta with ~10 mg of sublimed SbI_3 and heated within a sealed silica jacket, as indicated. A pure but only microcrystalline product was obtained without significant transport. A sintering process would probably succeed here as it did with cobalt. Arc-melting in this system gave a product with a sharp pattern and cell dimensions 0.05 Å less than for the sample prepared by more appropriate means.

The lattice constants for Zr_5Sb_3Ni (Table III) are appreciably (~0.07 and 0.05 Å, respectively) larger than obtained[14] following the powder sintering of a mixture of the elements in an evacuated silica tube at 800 °C for up to 8 weeks (a = 8.530 (5) Å, c = 5.773 (5) Å, c/a = 0.677). No mention was made of the phase composition of the latter product. At least an incomplete reaction is strongly implied.

The nickel and the cobalt phases as well as the binary host all show weak temperature-independent paramagnetism typical of metallic materials.[21]

Copper. The sintering of a pressed pellet of powdered Zr, Sb, and Cu_2Sb gave a good result. The a lattice constant was clearly

(20) Boller, H.; Parthé, E. *Acta Crystallogr.* **1963**, *16*, 830.

(21) Garcia, E.; Ku, H. C.; Shelton, R. N.; Corbett, J. D. *Solid State Commun.* **1988**, *65*, 757.

(22) Kwon, Y.-U.; Sevov, S.; Corbett, J. D., *Chem. Mater.*, in press.

larger than measured after arc-melting. The earlier report[14] of this compound again listed distinctly smaller dimensions, $a = 8.526$ (7) Å and $c = 5.786$ (5) Å.

Zinc. This synthesis was a natural candidate for a zinc-fluxed reaction as described above for silicon, and a quantitative yield of Zr_5Sb_3Zn rods was obtained. The structural study (below) verified the expected arrangement and composition. The lattice constants for this presumed phase prepared at 800 °C[14] are smaller by 0.052 and 0.016 Å, respectively.

Ruthenium. A contrasting result to unsuccessful attempts with iron is the single-phase sample of Zr_5Sb_3Ru obtained after reactive sintering. The phase had been reported not to exist.[14]

Silver. This compound has been prepared from the elements both with the aid of an SbI_3 mineralizing agent at 1150 °C and under "neat" conditions at 1350 °C. The products were identical, judging from the Guinier patterns, and have the largest cell of any Zr_5Sb_3Z phase so far obtained.

Others. The syntheses of a number of other stoichiometric Zr_5Sb_3Z phases by the methods reported here have repeatedly failed, namely, for Z = Cr, Mn, and Fe by several routes and for Z = B and N by arc-melting alone. An iron-containing phase can be obtained by arc-melting, but the lattice constants are erratic,[23] and a substantial amount of excess antimony is present (presumably substituting on the same interestitial site), judging from subsequent SEM analyses.[22] A similar problem seemed to affect the products of iron-transport reactions with SbI_3, while reaction of "$Zr_5Sb_3Li_2$" with FeI_2 at 1100 °C was incomplete, consistent with the foregoing. A dominant second phase in these iron reactions (and the source of ferromagnetism[21]) is $ZrFe_2$, and with manganese and chromium, a W_5Si_3-type phase with partial substitution of Mn or Cr in the centered silicon position is present.[22]

A preliminary reaction involving gallium suggested this derivative could also be prepared. Exploratory results indicate Zr_5Sb_3In can probably be obtained from the corresponding indium-fluxed reaction.

The foregoing syntheses generally gave homogeneous, single-phase products when loaded with the stoichiometric amount of Z to make Zr_5Sb_3Z. We believe that substantially all of these are effectively line phases at 1000–1300 °C. This is strongly supported by subsequent synthetic results in related systems where the addition of only fractional amounts of Z gives only mixtures of isomorphous phases, viz., the empty host and the completely stuffed product. The situation has recently been discussed at some length for the Zr_5Sn_3–Zr_5Sn_3(Sn) pair.[24] Similar findings pertain to Zr_5Sn_3Z (Z = Al, Cu, Ga, Ge),[25] as well as La_5Ge_3Z (Z = C, P, Mn, Co, Ni).[26] Refinements of several crystal structures for Zr_5Sb_3Z (below), Zr_5Sn_3Z,[25] and La_5Ge_3Z[26] phases also support this generality. Indeed, Zr_5Sb_{3+x}[2] is the only contrary result we know.

Crystal Chemistry. The lattice dimensions, ratios, and volumes of the above phases (Table III) show that these are distinctive and different from compositions in the Zr_5Sb_{3+x} phase regions, $0.0 \le x \le 0.4$. This information, coupled with the virtually single-phase products obtained from nearly all reactions, is strong evidence for the indicated compounds. This conclusion is further supported by the consistent volume trends observed as well as the result of selected SEM and single-crystal studies.

Although detailed changes in structural parameters are known from only a few structural studies, some generalities and trends can be deduced from the cell data. The volume trends are illustrated in Figure 2 as a function of period and group. Particularly striking is the tighter bonding of the Zr_5Sb_3 host produced by interstitial carbon and oxygen. All other compounds form with distinct, although relatively small, expansions. Phases containing 3d transition metals uniformly exhibit the smallest c/a ratios and fairly constant volumes, the largest cells naturally being found on incorporation of Ru and Ag. On the other hand, marked

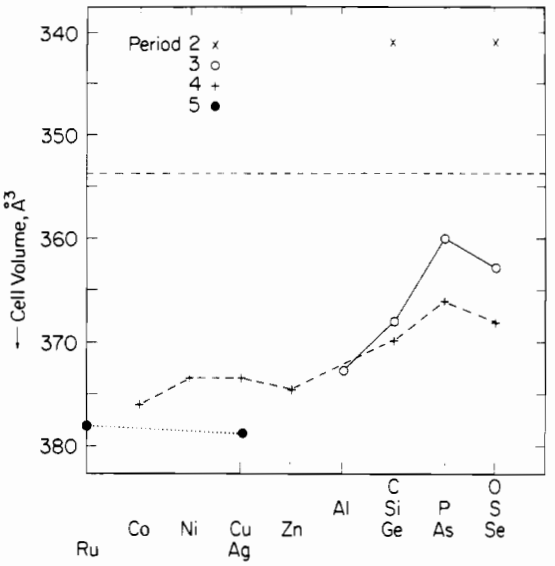

Figure 2. Unit cell volumes of Zr_5Sb_3Z (Å^3, increasing downward) as a function of period and group of Z. The dashed line marks the volume of the Zr_5Sb_3 host.

Table IV. Positional Parameters for Zr_5Sb_3Si and Zr_5Sb_3Zn

	x				B_{iso}, Å^2	
atom	Zr_5Sb_3Si	Zr_5Sb_3Zn	y	z	Zr_5Sb_3Si	Zr_5Sb_3Zn
Sb	0.60630 (8)	0.61504 (5)	0	1/4	1.10 (2)	0.54 (2)
Zr(1)[a]	1/3		2/3	0	1.03 (5)	0.48 (2)
Zr(2)	0.2619 (1)	0.27045 (7)	0	1/4	1.13 (4)	0.60 (3)
Si or Zn	0		0	0	1.4 (2)	0.48 (5)

[a] Zr(1) is the linear chain.

parallel decreases in volume and increases in c/a are discernible across the two series Al–S and Ge–Se, the members containing P, As and, more so, S, Se being the only ternaries to exhibit c/a ratios greater than that for the Zr_5Sb_3 host.

The marked increases in V and c at the end of these groups for both sulfur and selenium probably reflect a Coulombic repulsion between somewhat negatively charged chalcogens along the chain of clusters (Figure 1) since these interstitials are separated by just 2.95 Å ($c/2$). Although van der Waals diameters are not very realistic in such cases, an earlier survey of the literature[27] indicated that S···S and Se···Se closed-shell contacts in transition-metal chalcogenides were very tight and led to recognizable matrix effects when these fell near or below ~3.34 and 3.44 Å, respectively. (The minimum d(S–S) values in ZrS_2[28] and $Zr_{21}S_8$[29] are 3.66 and 3.41 Å, for instance.) The 2.95-Å separations in Zr_5Sb_3S and Zr_5Sb_3Se are in comparison very short indeed.

The volume changes seen in the Figure naturally reflect not only the presence of some free volume within the octahedral cavities in Zr_5Sb_3 but also substantial differences in effective interstitial volumes. Comparison of the standard atomic volume increments derived by Biltz[30] with these data show rather divergent behaviors. The transition metals produce expansions of 2 (Ag) to 5 (Co) Å^3 per formula unit relative to the standard increments of 7–10 Å^3, this difference falling to about zero with aluminum and then becoming negative by 5–10 Å^3 for all of the non-metals, carbon and oxygen excepted, of course. These differences seem contrary to the expected effects of coordination number alone, which for the standard volumes involve higher values for the metals and 4 or less for the non-metals. The bonding differences between the elements and interstitials must be responsible.

(23) Garcia, E. Ph.D. Dissertation, Iowa State University, 1987.
(24) Kwon, Y.-U.; Corbett, J. D. *Chem. Mater.* **1990**, *2*, 27.
(25) Kwon, Y.-U.; Corbett, J. D. To be published.
(26) Guloy, A.; Corbett, J. D. To be published.
(27) Corbett, J. D. *J. Solid State Chem.* **1981**, *39*, 62.
(28) Brattås, L.; Kjekshus, A. *Acta Chem. Scand.* **1973**, *27*, 1290.
(29) Franzen, H. F.; Beineke, T. A.; Conard, B. R. *Acta Crystallogr.* **1968**, *B24*, 412.
(30) Biltz, W. *Raumchemie der festen Stoffe*; Leopold Voss Verlag: Leipzig, East Germany, 1934.

Table V. Selected Distances (Å) in Zr_5Sb_3Z (Z = Si, Zn)[a]

	Z			Z	
	Si	Zn		Si	Zn
Sb–1Zr(2)[b]	2.951 (1)	2.966 (1)	Zr(2)–2Z	2.671 (1)	2.747 (1)
Sb–2Zr(2)[b]	2.974 (1)	2.947 (1)	Zr(2)–1Sb[b]	2.951 (1)	2.966 (1)
Sb–4Zr(1)	3.008 (1)	3.046 (1)	Zr(2)–2Sb[b]	2.974 (1)	2.947 (1)
Sb–2Zr(2)	3.109 (1)	3.080 (1)	Zr(2)–2Sb	3.109 (1)	3.080 (1)
Sb–2Sb	3.422 (1)	3.527 (1)	Zr(2)–4Zr(1)	3.518 (1)	3.494 (1)
Sb–2Z	3.671 (1)	3.621 (1)	Zr(2)–4Zr(2)	3.664 (1)	3.733 (1)
			Zr(2)–2Zr(2)[b]	3.887 (2)	4.032 (1)
Zr(1)–2Zr(1)	2.897 (1)	2.918 (1)	Z–6Zr(2)	2.671 (1)	2.747 (1)
Zr(1)–6Sb	3.008 (1)	3.047 (1)	Z–2Z	2.8967 (4)	2.9181 (4)
Zr(1)–6Zr(2)	3.519 (1)	3.494 (1)	Z–6Sb	3.671 (1)	3.621 (1)

[a] Distances <4.1 Å and the number of equivalent neighbors. [b] Distance vector lies normal to $\vec{c}$.

Single-crystal structures were investigated for two phases grown from a zinc flux, Zr_5Sb_3Si and Zr_5Sb_3Zn. Some crystal and refinement data are given in Table I, while positional parameters and important distances are reported in Tables IV and V, respectively. Additional information on data collection and refinement as well as atom displacement parameters and the structure factor listings are available as supplementary material.

The refinements were generally very satisfactory. There are some rather small uncertainties about the fine details of the silicide, however. The Guinier-based lattice constants of the zinc-fluxed product each differ by about 0.03 Å from those for the single-phase product prepared by powder sintering (Table I vs III). SEM–EDX analyses of three single crystals showed no zinc and gave an average composition (relative to Zr) of $Zr_5Sb_{3.02}Si_{0.91}$, with the coefficients probably uncertain by $\sim\pm0.05$. Refinement of the occupancies of Zr(1), Sb and Si (along with their thermal ellipsoids) relative to full Zr(2) occupancy gave values of 0.976 (6), 0.972 (4), and 1.13 (2), respectively. These correspond to the composition $Zr_{4.95(1)}Sb_{2.92(1)}Si_{1.13(2)}$ with no atom substitutions. The deviations of the refined values from unity are only 4, 7, and 6.5 σ and, under the circumstances, we are inclined not to make too much out of these small differences. Substitution of $\sim$3.8% Si for Sb, and vice versa, would account well for their refinement results. (Zr_5Si_3 is known, and light-atom interstitials[31] are not necessary.[32]) The small deficiency of scattering found for Zr(1) in the linear string is without precedent in our experience. In contrast, the zinc compound seemed virtually ideal in this respect with refined occupancies of 1.008 (4) for Sb, 0.999 (6) for Zn, and 1.005 (5) for Zr(1), corresponding to the composition $Zr_{5.01(1)}Sb_{3.02(1)}Zn_{0.999(6)}$.

Changes in distances within the Zr_5Sb_3 host on incorporation of Z are quite nonuniform and are not well reflected by the lattice dimensions, judging from the three examples for which structural details are available, namely with Z = 0.16Sb,[2] Si, and Zn. (Extrapolation of the $Zr_5Sb_{3.16}$ results to the empty cluster with the aid of lattice constants suggests the dimensional differences are small, but some uncertainties are also introduced.) The 0.16Sb–Si–Zn sequence involves substantial expansion of the Zr(2) octahedra, d(Zr–Z) increasing first by 0.14 and then by 0.08 Å. These are accomplished largely by increase in the Zr(2)–Zr(2) distances *within* the shared triangular faces in the chains, 0.29 and 0.14 Å, respectively, while distances between these triangles (the unshared edges of the octahedra—Figure 1) increase by less, 0.10 and 0.07 Å. The latter come about largely from the expansion in the shared faces since all atoms in this structure have fixed z values, and there is only a small increase in c through this series (0.03 Å). The shared triangles expand via increases in both a and x for Zr(2), meaning that considerations of only changes in the a lattice dimension on inclusion of Z will generally understate the expansion of the octahedral cavity. A smaller increase in a and, likewise, in the separation between confacial chains occurs in part because the Zr(2)–Sb exo distance diminishes nearly 0.1 Å when the cavity is first filled and then remains fairly constant. Approximately opposite distance changes are seen in the edge bridging of the triangles, Zr(2)–2Sb. The irregular changes that accompany bonding of different interstitial atoms mean that cell volume changes may be poor indicators of the effective sizes of interstitial atoms.

Variations in the c dimensions are generally small except for contractions seen with C and O and the increases with Ag, S, and Se already discussed. The limited expansion of c appears to conserve the strong Zr(1)–Zr(1) bonding that is suggested by the short distances ($c/2$) along this string; these are 0.7–1.1 Å less than those in the confacial chain and correspond to bond orders of about unity. The interchain distances Zr(1)–Zr(2), in fact the next larger zirconium separations at $\sim$3.5 Å, represent the most direct coupling between the two types of chains and show only a small decrease of $\sim$0.025 Å at each step. The corresponding bond populations do not suggest these are particularly strong interactions, however (below).

Arc-Melting Problems. This method has been utilized for synthesis of high-melting intermetallics for many years, largely for reasons of speed and convenience. The method effectively avoids nearly all of the container problems associated with the temperatures that are often necessary to gain equilibrium in sintering and related reactions. The value of single-crystal investigations in quantifying atom populations, distances, and, sometimes, compositions led to an emphasis on arc-melting methods for these T_5M_3Z systems in our earlier studies, since good whisker crystals often grow from the surface of the buttons in the final stages of solidification. On the other hand, suitable single crystals are rarely encountered from powder sintering reactions, at least under the conditions used here. However, much evidence is now available that neither the as-cast products nor the whisker crystals therefrom exhibit a very close relationship to the well-defined and generally stoichiometric phases achieved by reactions carried out in the neighborhood of 1000–1300 °C.

In all cases where sintering and arc-melting routes have both been examined (vide supra), the dimensions of the arc-melted products are distinctly smaller, and some are even close to those of Zr_5Sb_{3+x} samples. With Z = Al, Si, and Ga, the as-cast samples exhibit powder pattern lines that are additionally broad, distorted, or both, indicating a distribution of unit cell dimensions and thence compositions. The greater disorder associated with higher temperatures seems characteristic of this synthetic approach.

The Mn_5Si_3-type structure has been reported to occur with over 155 pairs of elements,[33] or more than 294 examples when ternary systems are included.[34] Many of the interstitials investigated here form analogous Zr_5Z_3 phase as well, and site exchange between Z and Sb at higher temperatures would not be surprising. The seemingly unique presence of self-interstitials in Zr_5Sb_{3+x} over the range $0 \le x \le 0.4$ (at $\sim$1100 °C)[2] also makes it easier to achieve off-stoichiometry through zirconium loss than if the host were a line phase. This deviation is especially favored when the particular Zr_5Sb_3Z ternary is unstable and either a ZrZ_n phase

(31) Nowotny, H.; Lux, B.; Kudielka, H. *Monatsh.* **1956**, *87*, 447.
(32) Kwon, Y.-U.; Rzeznik, M. A.; Guloy, A.; Corbett, J. D. *Chem. Mater.*, in press.
(33) Parthé, E.; Rieger, W. *J. Dental Res.* **1968**, *47*, 829.
(34) Villars, P.; Calvert, L. D. *Pearson's Handbook of Crystallographic Data for Intermetallic Phases*; American Society for Metals: Metals Park, OH, 1985; Vol. 1, p 580.

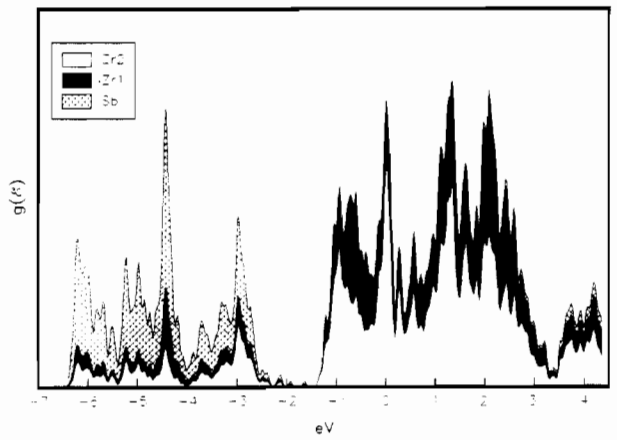

Figure 3. Density-of-states (DOS) diagram of the valence and conduction band region in Zr_5Sb_3 with atom contributions projected out. (Zr(2) occurs in the confacial chain; Sb 5s contributions are off the plot at higher binding energies.)

forms or Zr is lost into the Ta container, the latter becoming more serious at higher temperatures.[22]

A particularly serious problem with synthesis by arc-melting has been detailed for the Zr_5Sn_3–Zr_5Sn_4 system, the second phase being the self-interstitial (Ti_5Ga_4-type) version of the first. Not surprising, the two tin compounds, which are line phases near 1000 °C, appear to form a single solution phase at higher temperatures and eventually to melt congruently near 1800 °C and a composition $Zr_5Sn_{3.3}$.[24] These relationships produce a variety of complex powder pattern line shapes for as-cast samples in this composition region, not unlike some seen in the present study. The evident inhomogeneities generally cannot be readily removed and ordered phases recovered from as-cast samples by annealing near 1000–1100 °C.[2,22,24]

Further evidence supporting the apparent nature of the problems caused by arc-melting has been recovered from single-crystal studies of several whiskers formed on cooling.[23] For "Zr_5Sb_3Al", the refined interstitial occupancy (at R = 1.7%) could be interpreted as 72% Al, the remainder Sb, while 13% Al appeared to be substituted on the antimony site in the host. With "Zr_5Sb_3S", the interstitial site was 70% occupied if only sulfur was presumed present (R = 4.0%, with c and c/a 0.04 Å and 0.05 less, respectively, than those from powder sintering reactions (Table III)). In the case of "Zr_5Sb_3Fe",[21] about one-third of the interstitial sites are occupied by antimony according to recent studies.[22] Very similar problems with diminished lattice constants and stoichiometry deviations via refined occupancies have also been encountered in structural studies of single crystals recovered from arc-melted Zr_5Sn_3Z samples for Z = Al, Fe, and Ga.[25]

Band Calculations and Bonding. Some additional understanding of the Zr_5Sb_3 host and its prolific interstitial chemistry are provided by the results of a few extended Hückel band calculations. These afford only a brief overview, and more extensive inquiries on the bonding are warranted. The density-of-states (DOS) diagram for Zr_5Sb_3 is shown in Figure 3 (E_F = 0) with the contributions of the Sb (5p) and each of the two types of Zr atoms (mainly 4d) projected out. (Bands from the 5s states of Sb lie lower and are quite unimportant.) Two features are immediately obvious: a broad valence band derived from strong covalent mixing of zirconium 4d and antimony 5p orbitals for both types of metal atoms (Zr(1) in the linear string, Zr(2) in the confacial chain) and a well-separated conduction band comprising substantially only zirconium 4d contributions from both atom types. Since the relatively low-lying valence levels of the isolated antimony atoms are all filled, 11 electrons per formula unit remain for the conduction band ($5 \times 4 - 3 \times 3 = 11$).

COOP curves,[35] viz., the relative bonding between specified atom pairs in Zr_5Sb_3 weighted according to overlap and as a function of energy, are given in Figure 4, for two types of Zr–Sb and four types of Zr–Zr interactions. As is common, these functions become significantly antibonding (negative) only at higher energies. The upper plots show that Zr–Sb bonding (and nonbonding Sb 5p) states account for nearly all of the valence band, there being only a small Zr(1)–Zr(1) contribution to the largest peak in the valence band. On the other hand, the occupied conduction band consists almost entirely of metal–metal bonding interactions, which are shown broken down into the contributions of four types of Zr–Zr interactions: Zr(1)–Zr(1) (solid line),

(35) Hughbanks, T.; Hoffmann, R. *J. Am. Chem. Soc.* **1983**, *105*, 3531.

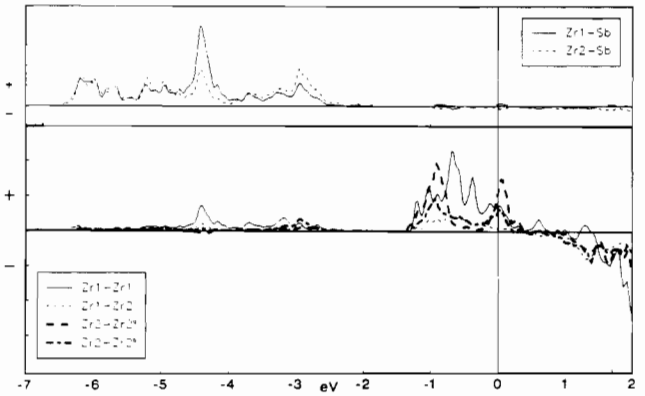

Figure 4. COOP (crystal orbital overlap population[35]) curves for the Zr–Sb and Zr–Zr interactions in Zr_5Sb_3, as marked: Zr(1)–Sb, solid line; Zr(2)–Sb, dashed line; Zr(1)–Zr(1) (isolated string), solid line; Zr(1)–Zr(2); (interchain), light dashed line; Zr(2)–Zr(2) in shared triangles, heavy dashed line; Zr(2)–Zr(2) between triangles, heavy dot–dash line.

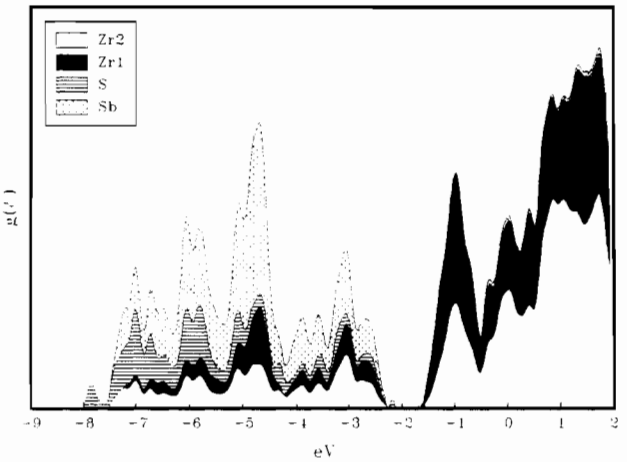

Figure 5. DOS results for Zr_5Sb_3S with the atom contributions projected out (occupied Sb 5s and S 3s states lie out of the region shown). Note the appearance of the low-lying Zr–S contributions in the valence band. (The smoothing factor used in this plot was twice that employed for Zr_5Sb_3 (Figure 3).)

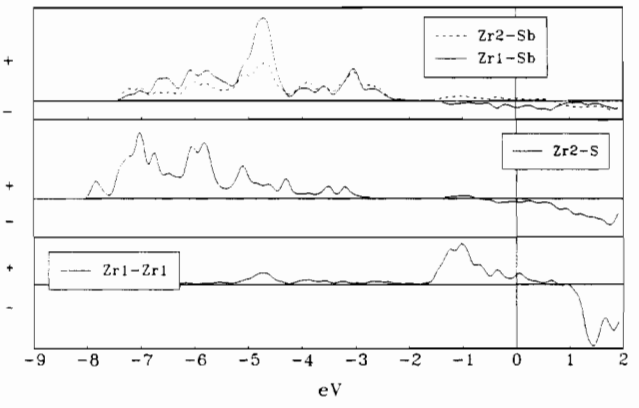

Figure 6. COOP curves for pair interactions in Zr_5Sb_3S: Zr–Sb (top); Zr(2)–S (middle); Zr(1)–Zr(1) (bottom). Note the similarity of the Zr–Sb portion to that in Zr_5Sb_3 (Figure 4) except for a shift to higher binding energy.

Table VI. Overlap Populations in Zr_5Sb_3 and Zr_5Sb_3S by Bond Type

	multiplicity (per formula unit)	Zr_5Sb_3	Zr_5Sb_3S
Zr(1)–Sb	12	0.28	0.30
Zr(2)–Sb	15	0.25	0.23
Zr(1)–Zr(1)	2	0.35	0.31
Zr(1)–Zr(2)	12	0.10	0.11
Zr(2)–Zr(2)[a]	3	0.17	0.02
Zr(2)–Zr(2)[b]	6	0.15	0.04
Zr–S	6		0.31
S–S	1		−0.07

[a] Within the triangles in the shared faces. [b] Between triangles.

Zr(1)–Zr(2) (dashed line), and the two types of Zr(2)–Zr(2), in the shared coplanar face (heavy dashed line) and between these triangles (heavy dash–dot). The relative magnitudes of these four curves provide quantitative measures of their significance.

The corresponding DOS and COOP data for Zr_5Sb_3S in Figures 5 and 6, respectively, indicate that considerable conceptual simplicity is associated with the incorporation of the third element, at least a fairly electronegative one. A broad component resulting from Zr(2)–S bonding appears on the high binding energy side of the virtually unchanged Zr–Sb valence band for the host. Some Zr(2) orbital population in the Zr_5Sb_3 conduction band as well as two electrons per sulfur are diverted into the sulfur valence band component while other, less bonding Zr(2) states are pushed higher in the conduction band. The result is a greater contribution of Zr(1) to the conduction band and a higher E_F relative both to the Zr(1)–Zr(1) bonding states in the lower region thereof and to the Zr–Sb valence band (compare Figures 3 and 5). Thus, the relatively weak Zr(2)–Zr(2) bonding in Zr_5Sb_3 is converted to Zr–S bonding with virtually no change in the Zr–Sb, Zr(1)–Zr(1), or Zr(1)–Zr(2) components of the host.

Integration of each of the atom projections in the DOS up to E_F give a rough estimate of electron populations and thence the "charge" on each, although the method is apt to overestimate polarities. Within this approximation, the introduction of sulfur and the accompanying small dimensional changes lead to a "charge" of −0.27 on S, while Zr(2) is naturally oxidized (0.25 → 0.54) as these atoms become involved in bonding to sulfur. This leaves Zr(1) relatively more reduced (0.20 → −0.07) in spite of the 0.13-Å lengthening of the Zr(1)–Zr(1) repeat but consistent with the relative change in the conduction band population (above). It is particularly satisfying to note that antimony, which with its strong bonding to both types of zirconium atoms provides much of the "glue" holding Zr_5Sb_3 and Zr_5Sb_3S together, is only slightly perturbed by the process, its apparent "charge" changing by a negligible amount (−0.38 → −0.40) on insertion of sulfur.

Overlap populations summed over occupied states (Table VI) give some succinct information regarding the process of sulfur encapsulation and quantify many of the effects inferred from Figures 3–6. Minor changes in Zr–Sb, Zr(1)–Zr(1), and Zr(1)–Zr(2) distances are all reflected in small changes in bond pair populations. In contrast, large effects accompany the replacement of both types of Zr(2)–Zr(2) bonding with Zr(2)–S bonds. An antibonding S–S interaction is calculated as well, appropriate to the 2.95-Å separation considered earlier. Of course, comparison of these populations for different types of atoms is not quantitative owing to changes in overlap integrals therewith, but a substantial increase in bonding and stability on sulfur inclusion is implied, and presumably this applied to many other Z examples as well.

Another useful comparison is found in the interchain Zr(1)–Zr(2) overlap populations, since these distances in Zr_5Sb_3Si and Zr_5Sb_3Zn are relatively short, 0.02–0.10 Å less than the Zr(2)–Zr(2) as well as Zr(1)–Zr(2) separations in the host. (Values in the sulfide will be close to those with silicon.) Notwithstanding, the Zr(1)–Zr(2) "bonds" between the two different zirconium chains in Zr_5Sb_3 have notably smaller overlap populations than for Zr(2)–Zr(2), pointing out the danger of inferring bond strengths only from distances and suggesting that a matrix effect,[27] namely the strong Zr(2)–Sb–Zr(1) interchain bridging, is probably more important than Zr–Zr bonding in determining the proximity of the two types of zirconium. In other words, appreciably more Zr(2)–Zr(1) states lie above E_F and are unoccupied. The magnitude of this particular population is quite unaffected on incorporation of sulfur (or iron).

A self-consistent-charge calculation was also carried out for Zr_5Sb_3Fe.[22] Although this turns out not to be a simple stoichiometric compound, the data provide a close approximation to the behavior of Zr_5Sb_3Co and Zr_5Sb_3Ni, and the general bonding characteristics provide a suitable contrast to the encapsulation of a non-metal. The charge-consistent 3d valence states now lie only 0.6–2 eV below Zr 4d, in contrast to a 5-eV gap between Zr 3d and S 3p, and there are naturally more orbitals on the interstitial. The Zr–Sb valence band is again scarcely perturbed in the process, but interstitial 3d along with Zr(2) now makes major contributions to the lower part of the conduction band, while the accompanying 4s states (together with Zr(2)) are mainly responsible for a narrow band that appears in the former gap.

Other Comparisons. Photoelectron spectroscopy data of the sulfide were also briefly examined. Unfortunately, the UPS (He I) results for Zr_5Sb_3S did not resolve the calculated band splitting although the broad valence band, a dip at about the calculated gap, and a clear Fermi edge were visible. Core-binding shifts determined by XPS (Al Kα) were more informative. The two types of zirconium atoms were not resolved, but their composite $3d_{5/2}$ binding energy, 179.5 eV, is reasonable in comparison with 178.5 eV in the metal,[36] considering that an overall oxidation has taken place in forming Zr_5Sb_3S. The $3d_{5/2}$ energy in elemental antimony, 528.1 eV,[37] is correspondingly reduced to 527.6 eV. Finally, the observed S $2p_{3/2}$ binding energy at 162.5 eV is seemingly reasonable in comparison with 163.8 eV in the element and 161.6 eV in Na_2S[38] although it is difficult to attach a great significance to particularly the sulfur trends because of the different location of the Fermi level references in the three materials.

These Zr_6Z cluster units show some interesting relationships relative to both binary ZrZ_n phases and centered zirconium cluster halides. In recent years, many examples of interstitial elements in isolated zirconium cluster halides have been discovered, viz., $M^I_x[Zr_6(Z)X_{12}]X_n$, where X covers Cl, Br, I and $0 \le x, n \le 6$.[3,4] The Zr–Z distances in the halides are quite reproducible among a variety of different compositions with fixed Z and X. The variables x, n in these cases are fairly well constrained by the evident need to come close to a closed-shell configuration in the cluster, e.g., 14 ± 1 e^- with main-group Z. This is in distinct contrast to the more electron-rich (metallic) $Zr_5M_3(Z)$ examples where electronic rules are not so restrictive, since differences are reflected largely in the conduction band populations, and a much greater variety of bound Z is possible. Notwithstanding, a regular trend in Zr–Z distances is encountered, as the zirconium in various types of Zr–Z systems is formally oxidized from ZrZ_n to Zr_5Sb_3Z to $Zr_6X_{12}(Z)$ units.

For interstitial silicon, comparative near-neighbor Zr–Si distances for a variety of binary phases ($ZrSi_2$, Zr_2Si, $ZrSi_2$, ZrCuSi) all fall in the range of 2.71–2.88 Å. The coordination number of zirconium vs silicon varies between 4 to 10 in this group and does not appear to be an important variable. The closest distances in the binary compounds are all greater than the d(Zr–Si) = 2.671 (1) Å in Zr_5Sb_3Si, which is in turn impressively greater than the 2.531 (2) Å distance in the halide cluster $Cs_{0.3}Zr_6(Si)I_{14}$.[39] Halide clusters containing zinc are not (yet) known, but 2.89–2.97 Å for Zr–Zn distances in ZrZn[40] and $ZrZn_2$[41] are likewise distinctly greater than 2.747 (1) Å in Zr_5Sb_3Zn. Similar differences in minimum T–Z distances between the two extremes, binary TZ_n phases and cluster halides, have been noted before for the com-

(36) Nefedov, V. I.; Salyn, Ya. V.; Chertkov, A. A.; Padurets, L. N. *Russ. J. Inorg. Chem. (Engl. Transl.)* **1974**, *19*, 1443.
(37) Shalvoy, R. B.; Fiusher, G. B.; Stiles, P. J. *Phys. Rev.* **1977**, *B15*, 1680.
(38) Lindberg, B. J.; Hamrin, K.; Johansson, G.; Gelius, U.; Fahlmann, A.; Nordling, C.; Siegbahn, K. *Phys. Scr.* **1970**, *1*, 277.
(39) Smith, J. D.; Corbett, J. D. *J. Am. Chem. Soc.* **1986**, *108*, 1927.
(40) Hansen, M. *Constitution of Binary Alloys*; McGraw-Hill: New York, 1958.
(41) Dwight, A. B. *Trans. Am. Soc. Met.* **1961**, *53*, 479.

binations Y-Ru,[42] Sc-Co,[43] Zr-Mn, Zr-Fe,[44] and Zr-P.[45] Compounds in the sequence ZrZ_n-Zr_5Sb_3Z-$Zr_6(Z)X_{12+n}$ involve the progressive oxidation of zirconium, and we imagine that the parallel removal of conduction band (or other) electrons that shield the bonding between Zr and Z is responsible for the inverse distance trend. It is evident that an unusual chemistry is operable in these systems.

Summary

The Zr_5Sb_3 example of the Mn_5Si_3 structure type exhibits a remarkable versatility in the variety of interstitial heteroatoms Z that may be bound within the confacial octahedra $^1_\infty[Zr_{6/2}Sb_{6/2}]$, for example, all elements in the fourth period from cobalt through selenium. The principal dimensional change taking place during these processes is the expansion of the zirconium octahedra within this chain, while the Zr-Sb distances show minimal variations. Electronically, the process of bonding Z within Zr_5Sb_3 converts some of the 11 approximately nonbonding electrons (per formula unit) and some Zr-Zr bonding states in the large conduction band into six strong Zr-Z interactions. This is accompanied by the partial loss of nine weaker Zr-Zr interactions in the octahedral chain, but with negligible alteration of the broad Zr-Sb-based valence band and the strong bonding of the Zr_5Sb_3 host reflected thereby. Each Zr_5Sb_3Z product is naturally thermodynamically stable with respect to the binary ZrZ_n phases that also exist for all examples of Z.

Acknowledgment. We are indebted to H. F. Franzen for the use of the arc-melting and some of the high-temperature vacuum equipment, to R. A. Jacobson for the X-ray diffractometer facilities, to J. W. Angeregg for the photoelectron data, to S. C. Sevov for SEM examinations, and to S. Wijeyesekera and T. Hughbanks for assistance and advice on the band calculations.

Supplementary Material Available: Tables of parameters for the single-crystal studies and the anisotropic atom displacement parameters in Zr_5Sb_3Si and Zr_5Sb_3Zn (2 pages); listings of observed and calculated structure factors for the same compounds (2 pages). Ordering information is given on any current masthead page.

(42) Hughbanks, T.; Corbett, J. D. *Inorg. Chem.* **1989**, *28*, 631.
(43) Hughbanks, T.; Corbett, J. D. *Inorg Chem.* **1988**, *27*, 2022.
(44) Hughbanks, T.; Rosenthal, G.; Corbett, J. D. *J. Am. Chem. Soc.* **1988**, *110*, 1511.
(45) Rosenthal, G.; Corbett, J. D. *Inorg. Chem.* **1988**, *27*, 53.

Contribution from the Departments of Chemistry, Energetics, and Organic Chemistry, University of Florence, Via Maragliano 75, I-50144 Florence, Italy

Selective Lithium Encapsulation in Aqueous Solution by the New Cage 4,10-Dimethyl-1,4,7,10,15-pentaazabicyclo[5.5.5]heptadecane (L). Synthesis, Characterization, and Structural Aspects. Crystal Structures of $[LiL][ClO_4]$ and $[CuL]Br_2 \cdot 3H_2O$

Andrea Bencini,[1a] Antonio Bianchi,[1a] Angela Borselli,[1a] Stefano Chimichi,[1b] Mario Ciampolini,[1a,*] Paolo Dapporto,[1c] Mauro Micheloni,[1a,*] Nicoletta Nardi,[1a] Paola Paoli,[1a] and Barbara Valtancoli[1a]

Received November 6, 1989

Synthesis and characterization of the new azamacrobicycle 4,10-dimethyl-1,4,7,10,15-pentaazabicyclo[5.5.5]heptadecane (L) are reported. The stepwise basicity constants have been determined by potentiometry (25 °C, 0.15 mol dm^{-3} NaCl). The azacage L behaves as a strong base (log K_1 = 12.48) in the first protonation step, as a much weaker base in the second step (log K_2 = 9.05), and as a very weak base in the last step (log $K_3 < 1$). The cage selectively encapsulates Li^+, and the inclusion $[LiL]^+$ complex formation equilibrium has been investigated by potentiometry (log K = 4.8) and ^7Li NMR techniques. The molecular structure of the complex $[LiL][ClO_4]$ has been determined by single-crystal X-ray analysis. The compound crystallizes in a monoclinic unit cell (space group $P2_1/n$) with lattice constants a = 15.046 (11) Å, b = 8.893 (4) Å, c = 15.305 (8) Å, and β = 113.58 (4)°, with Z = 4. Least-squares refinement converged at R = 0.065 for 1385 observed reflections of $I > 3\sigma(I)$. Li^+ is wholly enclosed in the cage cavity and adopts a five-coordinate geometry, with a short Li-N mean distance of 2.04 Å. The molecular structure of the complex $[CuL][Br_2] \cdot 3H_2O$ has been determined by single-crystal X-ray analysis. The compound crystallises in an orthorhombic unit cell (space group $Cmc2_1$) with lattice constants a = 11.629 (1) Å, b = 13.031 (1) Å, and c = 14.702 (1) Å, with Z = 4. Least-squares refinement converged at R = 0.068 for 542 observed reflections of $I > 3\sigma(I)$. The Cu^{2+} is enclosed by the cage and is five-coordinated, adopting a trigonal-bipyramidal coordination geometry. The electronic spectra of the copper complex show essentially the same features in the solid state and in solution and are diagnostic of five-coordinate trigonal-bipyramidal structures.

Introduction

Only in recent years attention has been paid to the coordination chemistry of alkali metals with nitrogen donor ligands.[2,3] Recently, we have synthesized a series of small azamacrobicycles, types of compounds that are highly preorganized molecules showing unusual basicity and complexing properties.[4-9] One of the interesting properties of some of these compounds is the selective Li^+ binding in aqueous solution, even in the presence of Na^+ excess.[4,6,8] With the aim of enhancing the Li^+ binding

(1) (a) Department of Chemistry. (b) Department of Organic Chemistry. (c) Department of Energetics.
(2) Constable, E. C.; Chung, L. Y.; Lewis, J.; Raithby, P. R. *J. Chem. Soc., Chem. Commun.* **1986**, 1719.
(3) Constable, E. C.; Doyle, M. J.; Healy, J.; Raithby, P. R. *J. Chem. Soc., Chem. Commun.* **1988**, 1262.
(4) Ciampolini, M.; Micheloni, M.; Vizza, F.; Zanobini, F.; Chimichi, S.; Dapporto, P. *J. Chem. Soc., Dalton Trans.* **1986**, 505.
(5) Ciampolini, M.; Micheloni, M.; Orioli, P.; Vizza, F.; Mangani, S.; Dapporto, P. *Gazz. Chim. Ital.* **1986**, *116*, 189.
(6) Bencini, A.; Bianchi, A.; Borselli, A.; Ciampolini, M.; Garcia-España, E.; Dapporto, P.; Micheloni, M.; Paoli, P.; Ramirez, J. A.; Valtancoli, B. *Inorg. Chem.* **1989**, *28*, 4279.
(7) Micheloni, M. *Comments Inorg. Chem.* **1988**, *8*, 79.
(8) Bencini, A.; Bianchi, A.; Ciampolini, M.; Garcia-España, E.; Dapporto, P.; Micheloni, M.; Paoli, P.; Ramirez, J. A.; Valtancoli, B. *J. Chem. Soc., Chem. Commun.* **1989**, 701.
(9) Bianchi, A.; Ciampolini, M.; Garcia-España, E.; Mangani, S.; Micheloni, M.; Ramirez, J. A.; Valtancoli, B. *J. Chem. Soc., Perkin Trans. 2*, **1989**, 1131.

0020-1669/90/1329-3282$02.50/0